

RESEARCH ARTICLE

Open Access



# Combined Color-Doppler Flow and Angio Planewave UltraSensitive™ Imaging for Analysis of Hemodynamic Characteristics of Normal Upper Limb Arteries

Yanzhou Liu<sup>1,4</sup>, Xiyue Zhang<sup>1,4</sup>, Hang Yang<sup>1,4</sup>, Xueyan Tan<sup>1,2,3,4</sup>, Duo Huang<sup>1,2,3,4</sup>, Hongmei Yuan<sup>1,2,3,4</sup>, Lili Yu<sup>1,4</sup>, Fang Yang<sup>1,2,3,4</sup>, Yuan Zou<sup>1,2,3,4</sup>, Xiuli He<sup>1,2,3,4</sup>, Yuqun Luo<sup>1,2,3,4</sup>, Fangzhao Cui<sup>1,4</sup>, Ping Wang<sup>1,2,3,4</sup>, Zukun Li<sup>1,2,3,4</sup>, Qing Zhang<sup>1,2,3,4</sup>, Ning Zhang<sup>1,2,3,4</sup>, Binglei Jiang<sup>1,2,3,4</sup> and Wensheng Yue<sup>1,2,3,4\*</sup>

## Abstract

**Background** To evaluate the hemodynamic characteristics of normal upper extremity arteries from the brachial artery to the fingertip arterioles.

**Methods** We analyzed the characteristics and changes in the regularities of ultrasonic parameters in the upper extremity arteries of 104 healthy volunteers using color Doppler flow imaging and Angio Planewave UltraSensitive™ imaging. The measured ultrasonic parameters included the vessel diameter, blood-flow spectrum waveform, peak systolic velocity, end-diastolic velocity, resistance index, pulsatility index, ratio of PSV to EDV, blood-flow volume, along with systolic acceleration of each BA, radial artery, superficial palmar arch artery, palmar proper digital artery, and third-grade artery arch of the fingernail bed.

**Results** From BA to FN3AA, the diameter, PSV, RI, S/D, VFlow, and slope of the artery significantly decreased ( $P < 0.001$ ), and size of the parameters significantly correlated with the anatomic position of the arteries. The blood-flow spectrum gradually changed from various waveforms to fixed monophasic waves. There was a linear relationship between the distribution of monophasic waveforms and arterial groups ( $R = -0.453$ ;  $P < 0.001$ ). When the blood-flow spectrum of BA and RA showed a monophasic waveform, their branch arteries showed the same. The waveforms of PPDA and FN3AA were also monophasic.

**Conclusion** Regular changes in the blood-flow spectrum waveform and hemodynamic parameters are related to the anatomic position of the upper limb arteries. CDFI combined with Angio PLUS accurately and systematically evaluates the hemodynamic characteristics of the upper extremity arteries.

**Keywords** Hemodynamic characteristic, Color-doppler flow spectrum, Upper limb artery, Brachial artery, Fingertip artery

†Yanzhou Liu, Xiyue Zhang, Hang Yang, Xueyan Tan have contributed equally to this work.

\*Correspondence:

Wensheng Yue  
yuepublic@163.com

Full list of author information is available at the end of the article



## 1 Background

Due of its non-invasive, convenient, and high practicability, color Doppler flow imaging has been widely used to detect peripheral arterial hemodynamics for several years [1–4]. The ultrasonic color Doppler spectrum characteristics of peripheral arteries are generally described as triphasic waveforms [4–7]. There are few accurate and in-depth analyses of the hemodynamics of upper extremity arteries in clinical practice, although they have shown various waveforms [8, 9].

A new and innovative paradigm which called Angio PLUS (Plane Wave UltraSensitive Imaging, SuperSonic Imagine, Aix-en-Provence, France), has been developed recently. Angio PLUS can provide more detailed information for microvascular flow by plane-wave continuous data sampling and three-dimensional wall filtering technology, which provides higher sensitivity and improved resolution for the clearly display of the extremely low velocity blood flow in small blood vessels [10, 19]. In this study, CDFI combined with Angio PLUS was used to systematically analyze the hemodynamic characteristics from the brachial artery level to the fingertip microcirculation in healthy adults. This was done to scrutinize the mechanisms, and influencing factors, to improve the understanding of existing hemodynamic theory of the upper extremity artery. To the best of our knowledge, this was the first study to focus on this aspect.

## 2 Materials and Methods

### 2.1 Participants and Clinical Characteristics

This study included 104 healthy adults (57 men, 47 women; age ranging between 27 and 70 years). All participants underwent basic clinical evaluations, including physical examination, blood pressure, routine blood, urine, blood lipid, blood sugar, liver function, kidney function, thyroid function, chest slices, heart and abdominal color ultrasound examinations. Patients with any type of vascular variation, acute and chronic infections, diabetes, hypertension, liver and kidney diseases, rheumatic and immune diseases, metabolic diseases, blood diseases, cardiovascular diseases, pregnant and lactating women were excluded from the study.

General information, such as age, sex, lifestyle, and past medical history were obtained. The results of physiologic and biochemical examinations were obtained from the clinical laboratory. Height and weight were manually measured to calculate the body mass index (BMI). The blood pressure of each subject was measured after sitting and resting for 20 min with a standard electronic sphygmomanometer (Omron HEM-7211, Matsuzaka, Japan). The final measurement results were based on the average of three measurements.

### 2.2 Procedure of Vascular Ultrasonography

In this experiment, an ultrasonic instrument (Hologic Supersonic Aixplorer, Provence, France) was used to detect the upper limb artery using a 4 to 15 MHz linear transducer (SL15-4). The operator had more than 3 years of experience in vascular ultrasound diagnosis, and was blinded to the participants' clinical characteristics. The temperature in the examination room was maintained between 23 and 25°C during the procedure. The participant was placed in a supine position, with a naturally extended upper limb and upward palm, and the whole arm was spread to the outside to achieve a 60° angle with the long axis of the body. Vascular ultrasonography was performed from the initial segment of the brachial artery to the fingertip arteriole.

For the analysis, brachial artery, radial artery, superficial palmar arch artery, palmar proper digital artery, and third-grade artery arch of the fingernail bed were divided into first to fifth artery groups, respectively. The BA and RA were detected by the use of CDFI, relatively, the SPAA, PPDA, and FN3AA were detected by the use of Angio PLUS. The vessels close to the heart were called proximal segment vessels, which are also termed as superior arteries.

### 2.3 Acquisition of Ultrasonic Parameters

For the larger vessels of the upper extremity, such as brachial and RA, the shape, wall, and color blood-flow signal filling of the vessels were detected by conventional two-dimensional ultrasound and CDFI. The diameter (D) of the cross-section of the BA was measured approximately 5–6 cm above the elbow, and the diameter of the RA was measured 2 cm above the transverse stria of the wrist. In the longitudinal section of the blood vessel, the pulse Doppler mode was used to obtain the arterial blood-flow spectrum. The sampling volume was placed in the center of the cavity set as  $\frac{1}{2}$ – $\frac{2}{3}$ rd of the inner cavity diameter, and the angle between the ultrasonic beam and lumen blood flow was adjusted to <60°. The Doppler spectrum waveform of each artery was observed and classified according to the different systolic and diastolic waveform manifestations. The mean hemodynamic parameters of three consecutive cardiac cycles in the blood-flow spectrum were measured, including peak systolic velocity, end-diastolic velocity, resistance index, pulsatility index, the ratio of PSV to EDV(S/D), time-averaged mean velocity, blood-flow volume, systolic acceleration.

The VFlow (the blood flow flowing through a certain section of the blood vessel every minute) was calculated using the formula,  $VFlow = \pi(D/2)^2 \times TAMV \times 60$ , in which TAMV was calculated automatically by the machine, and D was obtained manually. RI was calculated

using the formula,  $RI = (PSV-EDV)/PSV$ , and the mean RI of three consecutive cardiac cycles was automatically measured by the machine.

To demonstrate the tiny arteries of the hand in a better manner, a color power imaging model of Angio PLUS was used to acquire the blood-flow spectrum and hemodynamic parameters. The arteries examined in the hand included the SPAA, the proper palmar digital artery, and the third-grade artery arch of the FN3AA. During the examination, the right palm of the subject was placed upward, and the five fingers were separated. The skin surface of the site to be examined was coated with couplant and explored from the end of the ulnar artery. Since it was difficult to display the cross-section of arterioles, the lumen diameter and blood-flow spectrum waveform of arterioles were measured in the longitudinal section of the blood vessels. When the lumen blood-flow signal was adjusted without overflow, SPAA was detected approximately 2 cm close to the heart segment, PPDA in the middle phalangeal region, and the FN3AA in the radial side of the fingertip, and as is mention above that the Angio PLUS is highly sensitive to low-speed blood flow, when measuring the lumen diameter of microvasculature at the fingertips, the image was magnified 5 times to clearly display the lumen diameter of the vessel, and it was proceed manually in the sign area from the anterior to the posterior by the use of caliper tool. The measurement and recording method of the blood-flow spectrum parameters were the same as those of the BA. The measurement position of the finger artery is shown in the anatomical reference drawing (Fig. 1).

#### 2.4 Statistical Analysis

All statistical analyses were performed using the IBM SPSS 23.0 (International Business Machines Corporation, New York, America). Normality and homogeneity tests were performed for each continuous variable. Measurement data conforming to the normal distribution were expressed as  $\bar{x} \pm s$ , and those not conforming to the normal distribution were expressed as  $M(Q_R)$ . Count data were expressed as constituent ratios. Chi-square test was used to analyze the composition and distribution of various spectrum waveforms in each artery, and Mantel-Haenszel Chi-square trend test was used to evaluate the distribution trend of various spectrum waveforms among each artery. Kruskal-Wallis rank-sum test was used to compare the differences in measurement parameters between two or multiple groups of arteries. Spearman rank correlation coefficient was used to evaluate the correlation between arterial anatomic position and spectral waveform distribution. Statistical significance was set at  $P < 0.05$ .

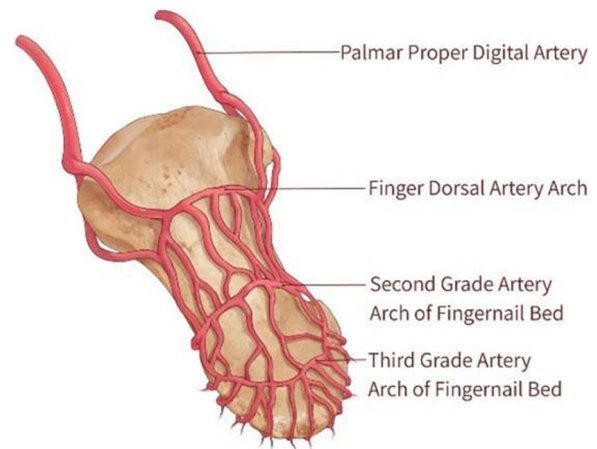


**Fig. 1** The specific measurement position of the PPDA, FN3AA is demonstrated in this anatomical reference drawing. (location for figure no.129)

#### 2.5 Patient and Public Involvement

Neither patients nor the public were involved in the design of the study and choice of outcome measures. Results of the study will be disseminated to subjects, the public and the scientific community.

### 3 Results

#### 3.1 Baseline Characteristics

The average age of 104 healthy adults was  $56.06 \pm 8.53$  years, and the average value of systolic pressure and diastolic pressure were  $129.89 \pm 13.69$  and  $82.41 \pm 9.57$  respectively, other characteristics like BMI and laboratory examination results were all recorded (Table 1).

#### 3.2 Distribution of Spectrum Waveforms of the Upper Limb Arteries

There were no significant difference in age between the sexes ( $t = 1.117$ ,  $P = 0.268$ ). The blood-flow spectrum waveforms of the bilateral upper limb arteries (208 BA, RA, SPAA, PPDA, and FN3AA) were divided into four types: monophasic waves, typical triphasic waves, atypical triphasic waves, and rare special waves (Fig. 2).

In this study, the three spectrum types, typical triphasic waves, atypical triphasic waves, and rare special waves along with diastolic reverse waves, were collectively referred to as non-monophasic waves. The distribution of monophasic waves and non-monophasic waves was different in BA, RA, SPAA, and PPDA (BA vs. RA  $\chi^2 = 66.555$ ,  $P < 0.001$ ; RA vs. SPAA  $\chi^2 = 5.562$ ,  $P = 0.018$ ; SPAA vs. PPDA  $\chi^2 = 10.246$ ,  $P = 0.001$ ), and the waveform distribution was related to the anatomic position of the artery (results of the Mantel-Haenszel Chi-square trend test:  $\chi^2 = 197.952$ , Spearman's test  $R = -0.453$ ,  $P < 0.001$ ).

**Table 1** Baseline characteristics [ $\bar{x} \pm s$  or  $n$  (%)] (location for no.151)

Demographics	(n = 104)
Age (years)	56.06 ± 8.53
Male	47(45.2)
Height (cm)	159.67 ± 7.04
Weight (kg)	60.71 ± 8.08
BMI	23.78 ± 2.64
Heart rate (beats/ minute)	66.72 ± 9.44
Systolic pressure (mmHg)	129.89 ± 13.69
Diastolic pressure (mmHg)	82.41 ± 9.57
Smoker	34(32.7)
Drinker	36(34.6)
Total cholesterol (mmol/L)	1.32 ± 0.34
Triglycerides (mmol/L)	4.39 ± 1.28
High-density lipoprotein cholesterol (mmol/L)	1.51 ± 0.60
Low-density lipoprotein cholesterol (mmol/L)	2.65 ± 0.79
Urea nitrogen (mmol/L)	4.23 ± 0.55
Creatinine (mmol/L)	61.24 ± 12.32
Fasting blood glucose (mmol/L)	5.07 ± 1.41
Alanine aminotransferase(U/L)	25.96 ± 8.58
Aspartate aminotransferase(U/L)	18.14 ± 6.75
Total protein(g/L)	71.32 ± 9.33
Albumin(g/L)	49.27 ± 6.94
Globulin(g/L)	21.53 ± 5.77
Albumin-globulin ratio	2.30 ± 0.46
Free triiodothyronine (pmol/L)	3.17 ± 0.54
Free thyroxine (pmol/L)	15.66 ± 5.01
Thyroid-stimulating hormone (μIU/ml)	3.35 ± 0.63

As the artery extended from the proximal to the distal end, the proportion of monophasic wave spectrum gradually increased. The blood-flow spectrum waveform of the finger arterioles (PPDA, FN3AA) was completely monophasic (Table 2).

### 3.3 Relationship Between the Spectrum Distribution of Different Arteries

When the blood-flow spectrum of the BA or RA showed a monophasic wave, the spectrum of their distal branch artery also showed a monophasic wave (Table 3).

### 3.4 Change in the Trend of Hemodynamic Parameters of the Upper Limb Artery

Arterial D, PSV, RI, PI, S/D, VFlow, and slope were compared among the five groups (BA, RA, SPAA, PPDA, and FN3AA), and the results showed statistically significant differences (Kruskal–Wallis tests  $H=980.569, 780.085, 690.868, 739.321, 635.824, 889.365, \text{ and } 863.741$ , respectively; all  $P < 0.001$ ). The above parameters were related to the anatomic position of the artery (Spearman's

$R = -.971, -0.856, -0.811, -0.841, -0.804, -0.924, \text{ and } -0.903$ , respectively; all  $P < 0.001$ ). From BA to FN3AA, the above parameters showed a decreasing trend (Fig. 3 and Table 4). There were significant differences in D, PSV, RI, PI, S/D, VFlow, and slope between arteries (BA vs. RA, RA vs. SPAA, SPAA vs. PPDA, and PPDA vs. FN3AA; all  $P < 0.05$ ) (Table 5). Significant differences in TAMV were observed between the arteries (SPAA vs. PPDA, PPDA vs. FN3AA and RA vs. PPDA; all  $P < 0.05$ ). There was a significant difference in EDV between the arteries (BA vs. RA, SPAA vs. PPDA, PPDA vs. FN3AA, BA vs. SPAA, RA vs. PPDA; all  $P < 0.05$ ).

## 4 Discussion

Since risk factors and population-aging trend are subject to change, the incidence of peripheral artery disease is projected to continue to increase over the next 20 years [11, 12]. According to previous studies, the risk of cardiovascular or cerebrovascular events in these patients has been reported to be 2–6 times higher compared to normal individuals [13]. Therefore, revealing and supplementing the changes in peripheral arterial hemodynamics would be helpful in the early prevention and treatment of cardiovascular diseases.

Several studies have described the characteristics of ultrasound hemodynamics of normal upper limb arteries as three-phase waveforms [4, 9]. An in-depth analysis of the hemodynamic ultrasound findings of normal upper limb arteries would be helpful in reducing missed clinical diagnoses of upper limb artery diseases, and also improve the early diagnosis rate. In this experiment, the latest ultrasound microvascular imaging technology-Angio PLUS. It is a newly paradigm that used in color Doppler domain. It used unfocused or plane waves and 3-dimensional wall filtering technology that can continuously offer higher frequency sampling for color flow imaging and extract the small vessels' blood flow using the 3-dimensional wall filtering to analyze the tissue motion in time, space and amplitude domain for the distinguishing of blood flow of microvessel and tissue, so that, we combined it with traditional high-frequency color Doppler ultrasound, and used them to systematically study the hemodynamic characteristics and changes in the trend of upper limb arteries in healthy adults (from BA to fingertip microvascular arteries). The results showed a decreasing trend in terms of extension of upper brachial artery to the distal limb, PSV, RI, PI, S/D, VFlow, and slope in the arterial lumen. The proportion of monophasic waves in the arterial blood-flow spectrum gradually increased (BA, 52.9%; RA, 88.9%; SPAA, 95.2%; PPDA, 100.0%), and the spectral waveform of PPDA and its distal micro-artery also showed monophasic waves.

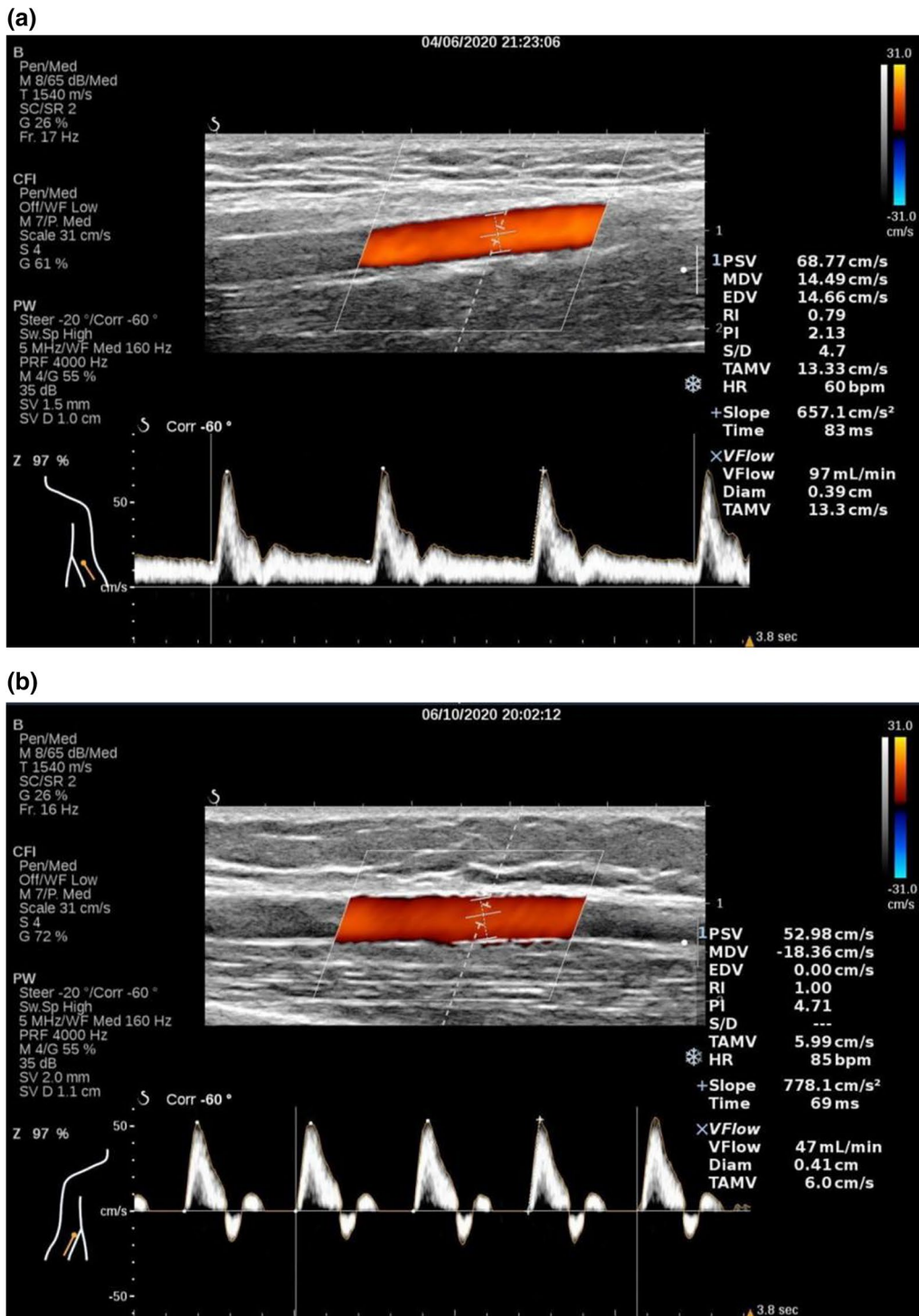


**Fig. 2** a Spectral Doppler showing the monophasic wave of left brachial artery with homogeneous blood flow. (location for figure no.156). **b** Spectral Doppler showing the typical triphasic wave of right brachial artery and the well-defined contour and distribution. (location for figure no.156). **c** Spectral Doppler showing the atypical triphasic wave of right brachial artery due to the decreasing peripheral resistance. (location for figure no.156). **d** A rare special wave of right brachial artery was showed in Spectral Doppler. (location for figure no.156)

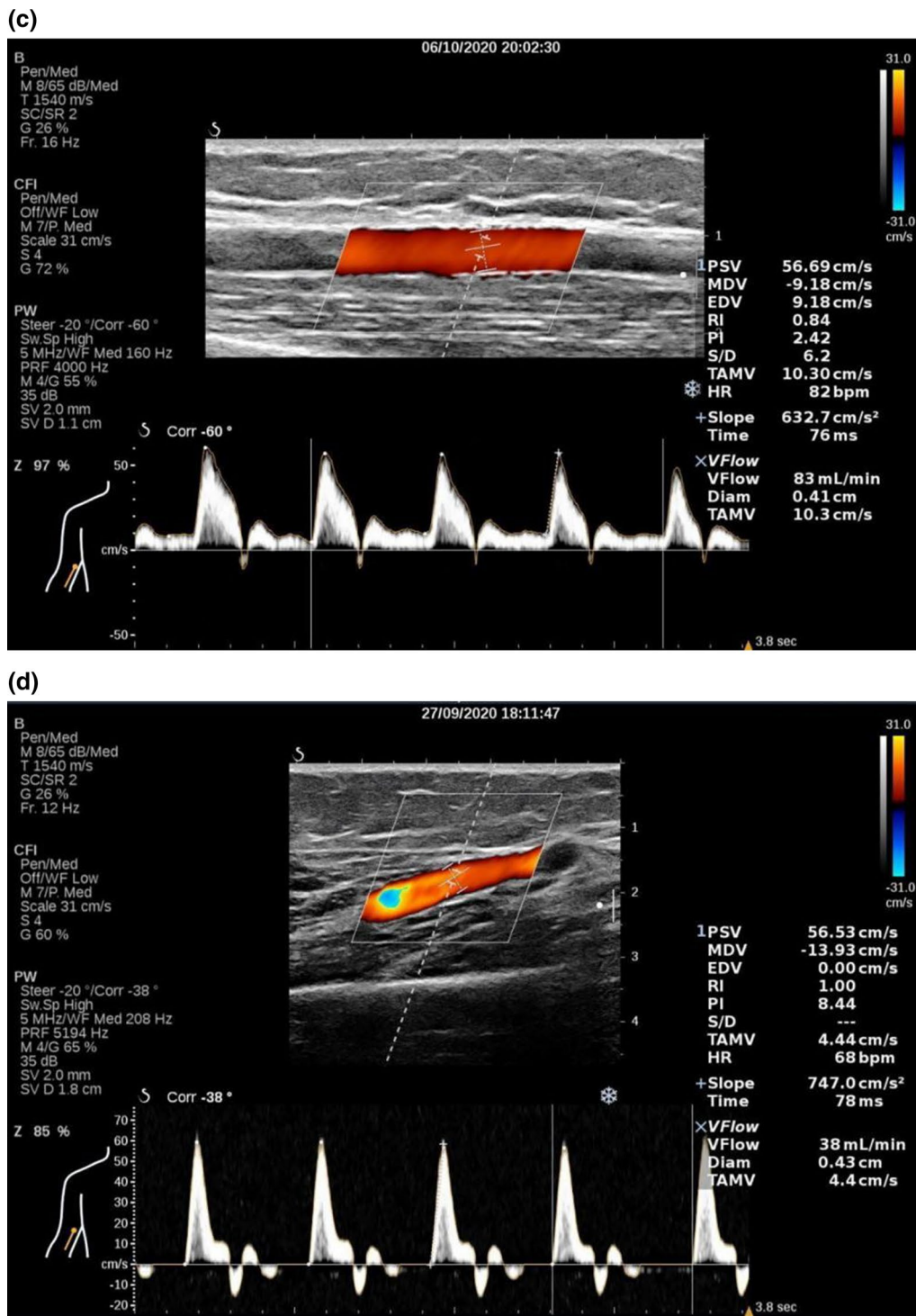


Fig. 2 continued

The flow of arterial blood is influenced by various forces. The pressure load generated by the heart pumping blood and elastic retraction force of blood vessel wall are the main driving forces of blood flow, whereas peripheral

artery resistance is the most important blood-flow resistance. Compared to the monophasic blood-flow spectrum waveform, the non-monophasic reverse wave appeared in the early diastole. This waveform represents a transient

**Table 2** Various waveform distributions of the upper limb arteries in healthy adults [n = 208, cases (%)] (location for no.166)

Group	Monophasic	Typical triphasic	Typical triphasic	Rare special	Non-monophasic	$\chi^2$	P value
BA	110 (52.9)	44 (21.2)	51 (24.5)	3 (1.4)	98 (47.1)	66.555	<0.001*
RA	185 (88.9)	16 (7.7)	7 (3.4)	0 (0)	23 (11.1)	5.562	0.018#
SPAA	198 (95.2)	6 (2.9)	4 (1.9)	0 (0)	10 (4.8)	10.246	0.001\$
PPDA	208 (100.0)	0 (0)	0 (0)	0 (0)	0 (0)	-	-
FN3AA	208 (100.0)	0 (0)	0 (0)	0 (0)	0 (0)	-	-

Analysis results of monophasic wave and non-monophasic wave distribution between arteries: \*P compared with the RA group. #P, compared with the SPAA group. \$P, compared to that of the PPDA group

BA brachial artery; FN3AA third-grade artery arch of fingernail bed; n number of arteries; PPDA proper palmar digital artery; RA radial artery; SPAA superficial palmar arch artery

**Table 3** Relationship between the spectrum distribution of different arteries [n = 208, cases (%)] (location for no.169)

Artery group		BA		RA	
		Monophasic	Non-monophasic	Monophasic	Non-monophasic
RA	Monophasic	110 (52.9)	75 (36.0)	-	-
	Non-monophasic	0 (0)	23 (11.1)	-	-
SPAA	Monophasic	110 (52.9)	88 (42.3)	185 (88.9)	13 (6.3)
	Non-monophasic	0 (0)	10 (4.8)	0 (0)	10 (4.8)

BA brachial artery; n number of arteries; RA radial artery; SPAA superficial palmar arch artery

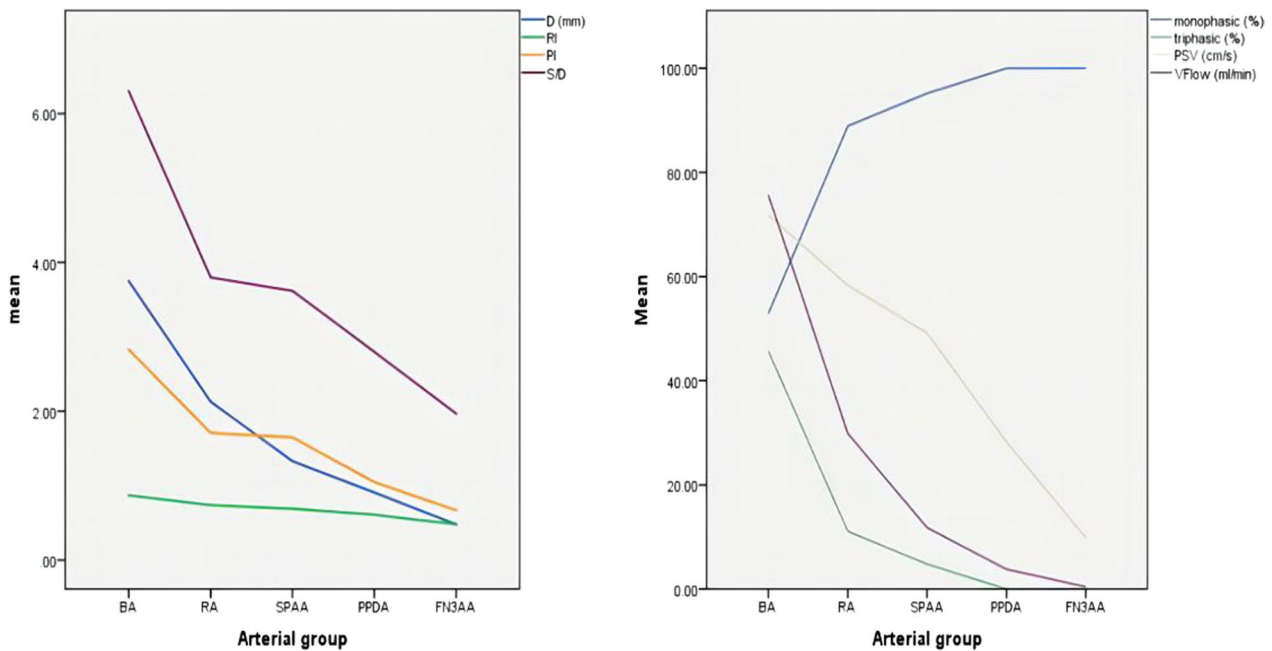


**Fig. 3** Trend of ultrasonic hemodynamic parameters of upper limb artery showed that from the BA to FN3AA, the vessel diameter, RI, PI, S/D, VFlow and PSV had a decreasing trend, however, the frequency of monophasic wave was on the increase. (location for figure no.177)

reverse flow of blood during early diastole. In some studies, the sphygmomanometer cuff was used to put pressure on the distal artery of the upper limb to simulate “peripheral vascular resistance”. Blood flow in the lumen

of the proximal artery was reversed in diastole, and the amplitude of the reverse spectrum waveform increased with an increase in the cuff pressure [6, 14]. This showed that the early reverse wave of arterial relaxation was

**Table 4** Anatomy and hemodynamic parameters of the upper limb artery in healthy adults [ $\bar{x} \pm s$  or  $M(Q_p)$ ] (location for Table no.177)

Artery groups	D (mm)	PSV (cm/s)	EDV (cm/s)	RI	PI	S/D	TAMV (cm/s)	Slope (cm/s <sup>2</sup> )	VFlow (ml/min)
BA	3.75±0.52	71.81±15.41	9.22 (10.79)	0.87 (0.15)	2.83 (1.51)	6.30 (4.52)	11.69±5.02	738.90±186.45	75.67±37.40
RA	2.13±0.35	58.33±16.13	14.96(12.05)	0.74(0.14)	1.71(0.98)	3.80(1.93)	12.71±6.23	553.40±150.83	29.88±19.85
SPAA	1.33±0.23	49.15±15.69	15.99±8.24	0.69±0.11	1.65±1.20	3.62±1.87	13.02±5.72	437.46±156.65	11.79±7.22
PPDA	0.91±0.14	28.24±12.24	11.80±8.34	0.61±0.10	1.05±0.34	2.80±1.01	9.00±4.45	164.70±82.35	3.80±2.31
FN3AA	0.48±0.09	9.83±3.85	5.11±2.10	0.48±0.07	0.67±0.15	1.97±0.31	3.60±1.38	26.40±14.56	0.42±0.49

BA brachial artery; D diameter; EDV end-diastolic velocity; FN3AA third-grade artery arch of fingernail bed; PI pulsatility index; PPDA proper palmar digital artery; PSV peak systolic velocity; RA radial artery; RI resistance index; Slope systolic acceleration; S/D ratio of PSV to EDV; SPAA superficial palmar arch artery, TAMV time-averaged mean velocity; VFlow, blood-flow volume

**Table 5** Comparative analysis of ultrasonic parameters between the upper limb arteries (location for no.179)

Parameters	BA vs. RA		RA vs. SPAA		SPAA vs. PPDA		PPDA vs. FN3AA		BA vs. SPAA		RA vs. PPDA	
	H	P value	H	P value	H	P value	H	P value	H	P value	H	P value
D(mm)	5.996	<0.001	6.065	<0.001	5.447	<0.001	10.976	<0.001	12.062	<0.001	11.513	<0.001
Psv(cm/s)	4.273	<0.001	3.314	0.001	8.313	<0.001	9.929	<0.001	7.586	<0.001	11.627	<0.001
Edv(cm/s)	-6.672	<0.001	-1.613	0.107	5.086	<0.001	10.488	<0.001	-8.285	<0.001	3.472	0.001
RI	6.244	<0.001	4.418	<0.001	5.451	<0.001	9.256	<0.001	10.662	<0.001	9.868	<0.001
PI	5.640	<0.001	4.462	<0.001	6.679	<0.001	9.068	<0.001	10.095	<0.001	11.154	<0.001
S/D	6.052	<0.001	4.050	<0.001	5.270	<0.001	9.674	<0.001	10.011	<0.001	9.278	<0.001
Tamv(cm/s)	-0.759	0.448	-0.873	0.382	6.285	<0.001	12.290	<0.001	-1.632	0.103	5.412	<0.001
Slope(cm/s <sup>2</sup> )	4.462	<0.001	3.601	0.005	9.010	<0.001	10.165	<0.001	8.064	<0.001	12.612	<0.001
Vflow(ml/min)	5.663	<0.001	5.269	<0.001	5.965	<0.001	10.357	<0.001	10.932	<0.001	11.234	<0.001

BA brachial artery; D diameter; EDV end-diastolic velocity; FN3AA third-grade artery arch of fingernail bed; PI pulsatility index; PPDA proper palmar digital artery; PSV peak systolic velocity; RA: radial artery; RI resistance index; Slope: systolic acceleration; S/D ratio of PSV to EDV; SPAA:superficial palmar arch artery; TAMV time-averaged mean velocity; VFlow blood-flow volume

mainly related to peripheral resistance [4]. This study also confirmed that with the normal upper limb artery extending from proximal to distal segment, the arterial blood flow RI and the display of early diastolic reverse wave in the blood-flow spectrum waveform decreased gradually.

The ultrasonic hemodynamic parameters of upper limb arteries show regular gradient changes with changes in the arterial anatomical position, which may be related to the difference in tissue metabolism levels at different anatomic positions. To improve the efficiency of local blood circulation, the vascular tension regulation of functional cells in the pipe wall of the blood supply artery is compensated to expand the blood vessels, thereby reducing blood-flow resistance [15, 16]. When blood-flow resistance in the lumen is lower than the vasodilation pressure, the arterial blood flows continuously forward in systole and diastole, and its blood-flow spectrum waveform displays a monophasic wave [17]. In an arm-controlled exercise experiment, it was observed that the diastolic blood-flow velocity of brachial artery was higher than that before exercise, and the blood-flow spectrum

waveform changed from triphasic wave to monophasic wave. This may be related to the tissue promoting compensatory regulation of vascular tension after muscle exercise to accelerate blood circulation [9].

To the best of our knowledge, this was the first study to demonstrate that when the blood-flow spectrum of BA, RA, or SPAA displayed a monophasic waveform, its distal extension artery also showed a monophasic waveform. This has not been mentioned in previous studies of upper limb arteries [18]. From the upper arm to forearm and the fingers, structure and function of local tissues of the upper limb are gradually refined and complicated, and the demand for metabolic levels also gradually increases. The regulatory effect of local arterial vascular functional cells is enhanced to accelerate blood circulation in the lumen. Therefore, the blood-flow spectrum of the upper limb artery shows a monophasic waveform from the proximal to the distal segment.

This study had several limitations. First, the sample size of this experiment was small, and the majority of study subjects were local residents of Nanchong City. Second, currently there is no standard quantitative reference



index for judgment of peripheral arterial blood-flow mechanics. Third, measuring blood-flow spectrum using ultrasound instruments is affected by multiple factors, which makes errors unavoidable. Last but not least, when measuring the lumen diameters of the arteries, we used two sections i.e., cross-section and longitudinal section to acquire the parameters, this might lead to measurement error and system error.

## 5 Conclusion

The ultrasonic blood-flow spectrum of the upper limb arteries in healthy adults showed various forms, and the distribution of the blood-flow spectrum between the upper and lower arteries was correlated. When extending from large proximal artery to small distal artery, the arterial blood-flow spectrum gradually showed a monophasic waveform, and the hemodynamic parameters showed a regular gradient trend. Thus, conventional high-frequency CDUS combined with Angio PLUS technology can be used to monitor the hemodynamic status of different arterial levels of the upper limb, to provide an early diagnostic basis for evaluation of peripheral arterial structural and functional lesions.

### Abbreviations

CDFI	Color doppler flow imaging
Angio PLUS	Angio planewave ultraSensitive™ imaging
D	Diameter
PSV	Peak systolic velocity
EDV	End-diastolic velocity
RI	Resistance index
PI	Pulsatility index
S/D	The ratio of PSV to EDV
VFlow	Blood-flow volume
TAMV	Time-averaged mean velocity
CPI	Color power imaging
BA	Brachial artery
RA	Radial artery
SPAA	Superficial palmar arch artery
PPDA	Palmar proper digital artery
FN3AA	Third-grade artery arch of the fingernail bed

### Acknowledgements

We thank the Health Management of the Affiliated Hospital of North Sichuan Medical College for providing the relevant clinical examination information of healthy volunteers. We also thank all the participants who volunteered for this study.

### Author Contributions

Contributors Tan XY, Huang D, Yuan HM and Yue WS contributed to the conception and design of the study. Tan XY, Liu YZ, Zhang XY, Yang H, Yu LL, Yang F, Zou Y, He XL, Luo YQ, Cui FZ, Wang P, Li ZK, Zhang N, Zhang Q, Jiang BL, Huang D, Li ZK and Yue WS contributed to the acquisition of data. Data analysis and interpretation were conducted by Tan XY and Yue WS. Tan XY and Yue WS wrote first draft of the protocol. Huang D revised the protocol critically for important intellectual content. All authors read and approved the final manuscript.

### Funding

This study was supported by Basic Application Foundation of Science and Technology Department of Sichuan Province (19YYJC0378) and Open Competition Mechanism to Select the Best Candidates of Affiliated Hospital of North Sichuan Medical College (2022JB001).

### Data Availability

Data are available upon reasonable request. The data that support the findings of this study are available from corresponding author, which were used under license for the current study and are not publicly available.

### Declarations

#### Ethical Approval

This study involves de-identified data of human participants and was approved by the ethics committee of the Affiliated Hospital of the North Sichuan Medical College, reference number 2020ER191-1, and followed the Declaration of Helsinki Ethical Principles for Medical Research Involving Human Subjects.

#### Consent for Publication

Verbal informed consent was obtained from the patient for their anonymized information to be published in this article.

#### Author details

<sup>1</sup>Department of Ultrasound, Affiliated Hospital of North Sichuan Medical College, Nanchong, China. <sup>2</sup>Academician Workstation, Affiliated Hospital of North Sichuan Medical College, Nanchong, China. <sup>3</sup>Medical Imaging Key Laboratory of Sichuan Province, Nanchong, China. <sup>4</sup>Nanchong Key Laboratory of Medical Ultrasound Engineering, Nanchong, China.

Received: 30 December 2023 Accepted: 15 April 2024

Published online: 21 May 2024

### References

- Conte MS, Bradbury AW, Kolh P, et al. Global Vascular Guidelines on the Management of Chronic Limb-Threatening Ischemia. *J Vasc Surg.* 2019;58(1):S1–109.
- Guirro E, Leite G, Dibai-Filho AV, et al. Intra- and Inter-Rater Reliability of Peripheral Arterial Blood Flow Velocity by Means of Doppler Ultrasound. *J Manipulative Physiol Ther.* 2017;40:236–40.
- Rangankar VP, Taori KB, Mundhada RG, et al. Accuracy of Common Femoral artery Doppler Waveform Analysis in Predicting Haemodynamically Significant Aortoiliac Lesions. *J Clin Diagn Res.* 2016;10(2):TC26–8.
- Nuffer Z, Rupasov A, Bekal N, et al. Spectral Doppler Ultrasound of Peripheral Arteries: a Pictorial Review. *Clin Imaging.* 2017;46:91–7.
- Li J, Karmakar MK, Li X, et al. Regional Hemodynamic Changes After an Axillary Brachial Plexus Block: a Pulsed-Wave Doppler Ultrasound Study. *Reg Anesth Pain Med.* 2012;37:111–8.
- Charlton PH, Mariscal Harana J, Vennin S, et al. Modeling Arterial Pulse Waves in Healthy Aging: a Database for in Silico Evaluation of Hemodynamics and Pulse Wave Indexes. 2019;317(5):H1062–85.
- Zócalo Y, Gómez-García M, Torrado J, et al. Aging-Related Moderation of the Link Between Compliance With International Physical Activity Recommendations and the Hemodynamic, Structural, and Functional Arterial Status of 3,619 Subjects Aged 3–90 Years. *Front Sports Act Living.* 2022;4:800249.
- Zubair A, Lotfollahzadeh S. Peripheral Arterial Duplex Assessment, Protocols, and Interpretation. In: *StatPearls.* Treasure Island (FL): StatPearls Publishing. 2023.
- Ozcan H, Oztekin PS, Zergeroğlu AM, et al. Doppler Ultrasound Evaluation of the Structural and Hemodynamic Changes in the Brachial Artery Following Two Different Exercise Protocols. *Diagn Interv Radiol.* 2006;12:80–4.
- Liu H, Liao Q, Wang Y, et al. A New Tool for Diagnosing Parathyroid Lesions: Angio Plus Ultrasound Imaging. *J Thorac Dis.* 2019;11:4829–34.
- Parvar SL, Fitridge R, Dawson J, et al. Medical and Lifestyle Management of Peripheral Arterial Disease. *J Vasc Surg.* 2018;68:1595–606.
- Campia U, Gerhard-Herman M, Piazza G, et al. Peripheral Artery Disease: Past, Present, and Future. *Am J Med.* 2019;132:1133–41.
- Dua A, Lee CJ. Epidemiology of Peripheral Arterial Disease and Critical Limb Ischemia. *Tech Vasc Interv Radiol.* 2016;19:91–5.
- Mouser JG, Ade CJ, Black CD, et al. Brachial Blood Flow Under Relative Levels of Blood Flow Restriction is Decreased in a Nonlinear Fashion. *Clin Physiol Funct Imaging.* 2018;38:425–30.

15. Tykocki NR, Boerman EM, Jackson WF. Smooth Muscle Ion Channels and Regulation of Vascular Tone in Resistance Arteries and Arterioles. *Compr Physiol*. 2017;7:485–581.
16. Hill MA, Meininger GA. Small Artery Mechanobiology: Roles of Cellular and Non-Cellular Elements. *Microcirculation*. 2016;23:611–3.
17. Wood MM, Romine LE, Lee YK, et al. Spectral Doppler Signature Waveforms in Ultrasonography: A Review of Normal and Abnormal Waveforms. *Ultrasound Q*. 2010;26:83–99.
18. Shi Y, Zhang XZ, Yin ZY, et al. Color Doppler Ultrasonographic Findings of Forearm Artery in Normal Adult. *Applied Journal of General Practice*. 2008;6:88–9.
19. Jung HK, Park AY, Ko KH, et al. Comparison of the Diagnostic Performance of Power Doppler Ultrasound and a New Microvascular Doppler Ultrasound Technique (AngioPLUS) for Differentiating Benign and Malignant Breast Masses. *J Ultras Med*. 2018;37:2689–98.